A Pair of Membrane-Embedded Acidic Residues in the NuoK Subunit of *Escherichia coli* NDH-1, a Counterpart of the ND4L Subunit of the Mitochondrial Complex I, Are Required for High Ubiquinone Reductase Activity†

Marko Kervinen,‡ Jukka Pätsi,‡ Moshe Finel,*,§ and Ilmo E. Hassinen*,‡

Department of Medical Biochemistry and Molecular Biology, University of Oulu, P.O. Box 5000, FIN-90014 Oulu, Finland, and Viikki DDTC, Department of Pharmacy, University of Helsinki, P.O. Box 56, FIN-00014 Helsinki, Finland

Received September 4, 2003; Revised Manuscript Received November 17, 2003

ABSTRACT: The ND4L subunit of mitochondrial NADH:ubiquinone oxidoreductase (complex I) is an integral membrane protein that contains two highly conserved glutamates within putative trans-membrane helices. We employed complex I from *Escherichia coli* (NDH-1) to study the role of these residues by site-directed mutagenesis. The conserved glutamates of the NuoK subunit, E36 and E72, were replaced by either Asp or Gln residues, and the effects of the mutations on cell growth and catalysis of electron transfer from deamino-NADH to ubiquinone analogues were examined. Additional mutants that carried acidic residues at selected positions within this domain were also prepared and analyzed. The results indicated that two closely located membrane-embedded acidic residues in NuoK are essential for high rates of ubiquinone reduction, a prerequisite for the growth of cytochrome *bo*-deficient *E. coli* cells on malate as the main carbon source. The two acidic residues do not have to be on adjacent helices, and mutual location on the same helix, either helix 2 or 3, at an interval of three amino acids (about one turn of the putative helix), resulted in high activity and good growth phenotypes. Nevertheless, shifting only one of them, either E36 or E72, toward the periplasmic side of the membrane by about one turn of the helix severely hampered activity and growth, whereas moving both acidic residues together to that deeper membrane position stimulated the ubiquinone reductase activity of the enzyme but not cell growth on malate, suggesting impaired energy conservation in this mutant.

The H^+-translocating NADH:ubiquinone reductase (also called complex I in mitochondria and NDH-1 in bacteria) is a very large, complex membrane-bound enzyme that catalyzes the first electron-transfer reaction of the respiratory chain in most mitochondria and several bacteria (*1*−*5*). Complex I is composed of many protein subunits, and its redox centers are FMN and several Fe−S clusters (for recent reviews, see refs *6*−*11*). The size, complexity, and important functions of this enzyme, as well as the involvement of complex I deficiencies in many mitochondrial diseases, make it a challenging research object.

Mammalian complex I is located in the inner mitochondrial membrane and contains some 45 protein subunits, seven of which are encoded and synthesized within the organelle (*1*, *12*−*15*). The latter subunits, called ND1-ND6 and ND4L, form most of the membrane domain of the enzyme and are probably involved in the ubiquinone reduction and proton translocation activities of complex I. Mutations in these subunits (the NDs) may cause a number of neurodegenerative diseases (e.g., Leber's Hereditary Optic Neuropathy), which are typically maternally inherited (*16*). It is thus interesting to study the effect of mutations in the ND subunits on the structure, function, and assembly of complex I. Such an undertaking is hampered, however, by the enormous difficulties in introducing specific mutations into mitochondrially encoded proteins.

The bacterial enzymes, the NDH-1s, contain 14 protein subunits, or 13 in *Escherichia coli*, and some other bacteria in which the subunits NuoC and NuoD are fused into a single protein. Despite having a relatively low number of subunits and only about half the protein mass of eukaryotic complex I, the bacterial enzymes are similar in their activities of and redox center content to their fungal and mammalian counterparts (*17*−*19*). Hence, due to the accessibility of all the bacterial NDH-1 subunits to genetic manipulation (*20*), this is a very attractive system for studying the mitochondrial enzyme, particularly the subunits that are encoded by mitochondrial genes.

Acidic residues within trans-membrane helices of integral membrane proteins are rare and when found are often highly conserved (*21*, *22*). Such residues are expected to be directly involved in vectorial proton movements across the membrane (e.g., in the case of the c subunit (proteolipid) of ATP synthase, subunit I of cytochrome *c* oxidase, or other members of the heme-copper terminal oxidase protein family (*23*−*27*)). In the case of complex I, however, no such highly conserved and deeply membrane-embedded acidic residues

† This investigation was supported by the Academy of Finland Council of Health (Cell Biology Program) and the Sigrid Juselius Foundation.

* Corresponding authors. (M.F.) Tel.: +358-9-19159193. Fax: +358-9-19159556. E-mail: moshe.finel@helsinki.fi. (I.H.) Tel.: +358-8-5375802. Fax: +358-8-5375811. E-mail: ilmo.hassinen@oulu.fi.

‡ University of Oulu.

§ University of Helsinki.

10.1021/bi0355903 CCC: $27.50
Published on Web 12/30/2003

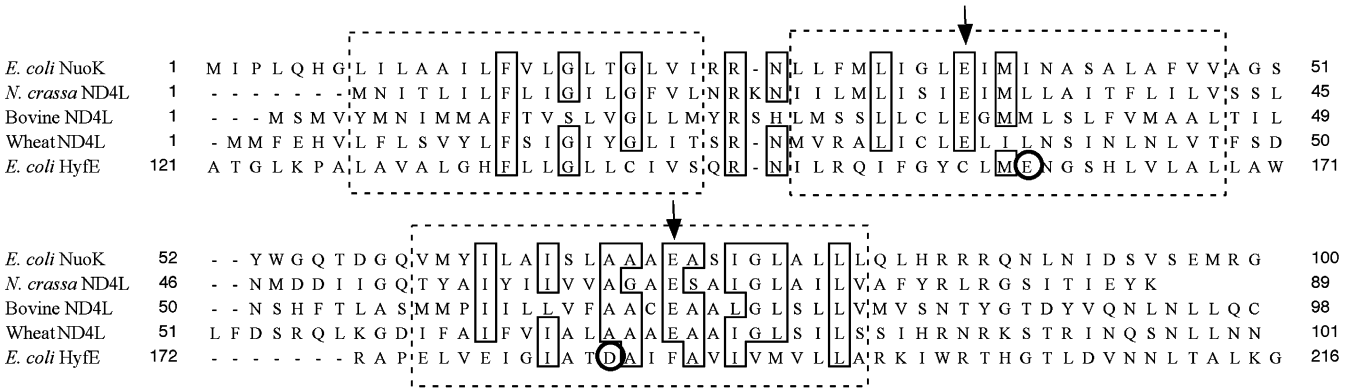

FIGURE 1: Alignment of the *E. coli* NuoK subunit with selected complex I homologues and with subunit E of the hydrogenase-4 of *E. coli*. Putative transmembrane helices are indicated by dashed lines. The two conserved glutamate residues (E36 and E72 in NuoK) are indicated by arrows, and their presumed hydrogenase equivalents are encircled. Accession numbers for the sequences: *E. coli* NuoK, NP_416782; *N. crassa* ND4L, P05509; bovine ND4L, NP_008103; wheat ND4L, O98694; and *E. coli* HyfE, NP_416980.

have so far been found within the integral membrane protein subunits thought to participate in ubiquinone binding, namely, ND1, ND2, ND4, and ND5 [NuoH, NuoN, NuoM, and NuoL in *E. coli* NDH-1, respectively] (*28*−*31*).

Di Bernardo and co-workers have reported that the pair of highly conserved acidic residues in the bacterial homologue of the ND3 subunit (Nqo7 in *Paracoccus denitrificans* or NuoA in *E. coli*) is probably located within a transmembrane helix (*32*). These residues, NuoA D79 and NuoA E81 in the case of *E. coli*, are preceded by a phenylalanine residue, NuoA F78, that appears to be even more conserved than D79. We have found three sequences (accession numbers CAA88774, D83410, and CAC08300) that seem to contain the equivalents of F78 and E81 but not of D79. It is currently unknown, however, whether these sequences represent functional ND3 homologues.

The ND4L subunit of complex I (NuoK in *E. coli*) contains two highly conserved Glu residues that are predicted to reside within trans-membrane helices 2 and 3 (Figure 1, see also ref *33*). In contrast to the acidic residue motif in NuoA (ND3, ref *32*), the two membrane-embedded Glu residues in NuoK are located on different helices (Figure 1). We have previously noticed that the second formatehydrogenlyase of *E. coli* (hydrogenase 4), the enzyme encoded by the Hyf operon (*34*), contains a subunit that is homologous to ND4L (*2*). Sequence alignment of HyfE and the NuoK subunit of *E. coli* NDH-1 reveals that HyfE also has two putative membrane-embedded acidic residues, E159 and D184, but they are shifted with respect to E36 and E72 of NuoK (Figure 1). E159 of HyfE is shifted three places toward the C-terminus, and D184 is shifted three places toward the N-terminus (Figure 1).

The homology between NuoK (and ND4L) and HyfE, and the observed shift in the position of the acidic residues (Figure 1), may suggest that the two membrane-embedded glutamate residues in NuoK are located on different helices and at the same depth inside the bilayer. Such an arrangement might mean that the two glutamate side chains are directed toward each other and are stabilized either by a divalent cation, if charged, or by hydrogen bonding. To test these working hypotheses, we deleted *nuoK* (together with *nuoJ*) from the bacterial genome, complemented the deletion in trans with *nuoJ* + *nuoK*, which carried different point mutations, and assessed the effects of the mutations on enzyme activity and cell growth in media that necessitate effective NADH oxidation.

Table 1: *E. coli* Strains and Parental Plasmids Used in This Study

strain or plasmid	relevant genotype	ref
GV102	F⁻ *hsdR*514 *supE*44 *lacY*1 *galK*2 *galT*22 *metB*1 *trpR*55 *supF*58, Δ*cyo::kan*	*35*
GVnuoJK	GV102, Δ*nuoJK::Sm*^{r}	this paper
GO103	F⁻ *thi rpsL gal zbg-2200::kan* Δ*cydAB′*	*35*
GOnuoJK	GO103, Δ*nuoJK::Zeo*^{r}	this paper
pJK	nuoJK-myc-his in pETBlue2	this paper
pJKwt	nuoJK in pETBlue2	this paper
pHN3	ndh-his in pQE−31	*36*

EXPERIMENTAL PROCEDURES

Materials. Decylubiquinone (DB),[1] NADH, deamino-NADH, DL-malate, *N*-vanillylnonanamide, and MES were from Sigma; disodium succinate was from Fluka; and sodium pyruvate was from Boehringer Mannheim. HAR was purchased from Aldrich, HEPES from AppliChem, and KCN and PMSF from Merck; and Q_2 was a generous gift from Eisai Corp., Japan. The annonin mixture was purchased from Dr. Y. K. Gupta, Varanasi, India. Oligonucleotides for the deletion were obtained from Gibco, and PAGE-purified oligonucleotides for mutagenesis were purchased from Sigma-Genosys. The QuikChange XL mutagenesis kit was from Stratagene. DIA900 anti-His-tag antibodies were from Dianova, and goat anti-mouse IgG HRP-conjugated antibodies were from BioRad. Genotypes of the parental bacterial strains (*35*, *36*) and plasmids are summarized in Table 1.

NuoJ Plus nuoK Deletion. The deletions were introduced essentially according to ref *37*. Vent DNA polymerase (New England Biolabs) was used in all the PCR amplifications. Regions flanking the intended *nuoJK* deletion were amplified using oligonucleotides 1−2 (Table 2, Figure 2) for the upper flank (UF) and 3−4 for the lower flank (LF). UF was ligated into EcoR5-EcoR1 sites of Litmus39 and LF separately into

[1] Abbreviations: d-NADH, deamino-NADH (nicotinamide-hypoxanthine dinucleotide (reduced form)); DB, decylubiquinone (2,3-dimethoxy-5-methyl-6-decyl-1,4-benzoquinone); HAR, hexammineruthenium; IPTG, isopropyl-β-D-thiogalactoside; MES, morpholinoethanesulfonic acid; PMSF, phenylmethylsulfonylfluoride; Q_2, ubiquinone-2; VNA, *n*-vanillylnonanamide.

Table 2: Oligonucleotides Used

Oligo	Sequence[a]	Restriction site
1) UFSmaF	caacatgcccgggatcgtcaacagcc	SmaI
2) UFEcoRIR	cattgcccgaattcttacggtaacagg	EcoRI
3) LFEcoRIF	gaacctgaacagaattccagtaagtgag	EcoRI
4) LFSalR	gtggaaagtcgacgcatcccatgc	SalI
5) UFF2	ccttgatgggcgtggtggcgcaggc	-
6) SmR2	gcccgtcgttgcctgatggatccc	-
7) SmF2	ctagcgagggctttactaagctcg	-
8) LFR2	ggaaccggatgccaggaacagcagcg	-
9) BJK1NcoF	gagaggggccatggagttcgc	NcoI
10) KEcoR	gcaagcatggaattccgcgcatctc	EcoRI
11) dHisF3	cagtaagtgagatgcgcggatgacgaagctttctagaacaaaaactc	-
12) K36QF3	gctgtttatgttgattggtctgcagatcatgattaacgcctcc	PstI
13) K36DF1	gctgtttatgttgattggtctggatatcatgattaacgcc	EcoRV
14) K72QF1	ccatcagcctcgcggctgcgcaagcgagtatcg	AviII
15) K72DF8	cgcggcggcagacgcgtctatcggccttgc	MluI
16) K39DF1	gattggtctggaaatcatggataacgcgtccgcgctggc	MluI
17) K39EF2	gttgattggtctggaaatcatggagaacgcgtccgcgctggc	MluI
18) K69DF1	cattctcgccatcagtctagacgcggcagaagcgagtatcgg	XbaI
19) K36Q39DF1	gattggtctgcagatcatggataacgcgtccgcgctggc	MluI
20) K36Q39EF2	gttgattggtctgcagatcatggagaacgcgtccgcgctggc	MluI
21) K72Q69DF1	cattctcgccatcagtctagacgcggcacaagcgagtatcgg	XbaI
22) ZeoSEF	aggcctgaattctgttgacaattaatcatcggcatag	StuI-EcoRI
23) ZeoSER	aggcctgaattcagtcctgctcctcggccac	StuI-EcoRI

[a] The restriction sites are underlined, and the mutated nucleotides are in bold. For the mutagenesis oligonucleotides, 13−21, only the forward one is shown, as the other one was reverse-complementary to it.

EcoR1-Sal1 sites, yielding pL39UF and pL39LF, respectively. LF was cloned as an EcoR1-Spe1 fragment into EcoR1-Nhe1-digested pL39UF, yielding pULF. The Sm^R gene from pSUP202mp6 (*38*) was isolated by EcoR1 digestion and inserted into the EcoR1 site between the upper and the lower flanks of *nuoJ* + *K* in pULF. A Stu1-Sal1 fragment of this construct was cloned into the Sma1-Sal1 site of pKO3, and gene replacement was performed according to ref *37*, except that a temperature of 42 °C was used instead of 43 °C. The correctness of the deletion was verified by PCR using primers from upstream of UF (oligo no. 5 in Table 2, Figure 2) and from inside the Sm^R gene (oligo no. 6 in Table 2) or primers from downstream of the LF (oligo no. 8 in Table 2) and from inside the Sm^R gene (oligo no. 7 in Table 2). The flanking regions were sequenced to confirm that no unwanted mutations had been introduced during the procedure. In the deletion construct for GO103, the Sm^R gene was replaced with the Zeo^R gene, which was amplified from the plasmid pPICZ-A (Invitrogen) using primer nos. 22 and 23.

NuoJ Plus nuoK Expression Construct and Mutagenesis. Expression plasmids for in trans complementation were prepared by amplifying the *nuoJ* + *K* fragment from genomic DNA using primers 9 and 10 (Table 2, Figure 2) and subcloning into pBAD-MycHisB (Invitrogen) digested with Nco1 plus EcoR1, generating pBJK. The Nco1-Dra1 fragment from pBJK, containing the BAD-derived myc-epitope tag, the polyhistidine tag, and the stop codon, was subcloned into pETBlue-2 digested with Nco1 plus EcoR5, generating the expression plasmid pJK. The sequence of the insert in pJK was verified by DNA sequencing. Point mutations were introduced into pJK using the QuikChange XL mutagenesis kit (Stratagene) according to the manufacturer's instructions, followed by DNA sequencing of the mutant gene. In the case of the E72Q mutant, an additional mutation, G34D, was found in addition to the desired one. This unplanned double mutant was nevertheless studied further since it provides an interesting control. The tetra-mutant E36Q/I39D/A69D/E72Q (QDDQ) was constructed by replacing the BsrG1 fragment of the E36Q/I39D mutant plasmid with the respective fragment from the E72Q/A69D plasmid.

Bacterial Growth and Membrane Preparation. Bacteria were grown routinely in the LB medium with appropriate antibiotics, apart from the growth experiments in minimal media that are described below. The malate-YE medium contained 65 mM potassium phosphate buffer supplemented with 0.1% (w/v) yeast extract, 1 mM citrate, 75 mM ammonium sulfate, 90 mM DL-malate, and salts (590 μM $MgSO_4$, 100 μM $CaCl_2$, 90 μM $FeCl_3$, 50 μM $MnCl_2$, 25 μM $ZnCl_2$, 5 μM H_3BO_3, 10 μM $CoCl_2$, 10 μM Na_2MoO_4), pH 7.1 (*31*). Malate was replaced by 45 mM succinate, 45 mM pyruvate, or 15 mM glycerol in the respective growth experiments. For membrane preparation, cells were recovered from glycerol stock overnight in LB in the presence of streptomycin and ampicillin (where applicable), diluted 1:100 in fresh LB or malate-YE medium (supplemented with ampicillin where applicable), and grown at 37 °C under high aeration. The cells were collected when the absorbance at 600 nm (A_{600}) reached 0.6−1, cooled, and washed with buffer A containing 50 mM MES, pH 6.5, 2.5 mM EDTA, and 0.2 mM PMSF. The washed cells were stored at −80 °C before further steps. Two methods were used for breaking the cells. Thawed cells were suspended in 10 mL of buffer A per gram of wet cells, and all subsequent steps were carried out either on ice or at 4 °C. Lysozyme, 0.15 mg/mL, was then added, and the suspension was placed on a shaker for 1 h, followed by 5-fold dilution with cold water and suspended by means of a Teflon pestle homogenizer. The membrane fraction was collected by ultracentrifugation (120 000*g*, 60 min) and suspended in buffer B (10 mM MES, pH 6.5, containing EDTA and PMSF as above) to about 2 mL per gram of initial cell weight. Optionally thawed bacteria were prepared according to ref *39*, except that buffer A was used during the French Press treatment, and the membranes were suspended in buffer B after ultracentrifugation (120 000*g*, 60 min). The protein concentration in the membrane preparations was assessed according to Lowry (*40*). The NDH-1 activities in the differently prepared membranes were practically identical (results not shown).

Enzyme Activity Measurements. The activity assays were performed using a Shimadzu UV-3000 spectrophotometer at 30 °C. NADH or deamino-NADH oxidation was followed in terms of the absorbance difference between 340 and 385 nm, and the initial activities were calculated using an extinction coefficient of 5.3 mM^{-1} cm^{-1}. Electron transfer from deamino-NADH to HAR was measured in the presence of 20 mM KCN, 1 μg/mL annonin, 2 mM HAR, 50 μM d-NADH, 16 mM HEPES, pH 7.8, and 6−30 μg of protein

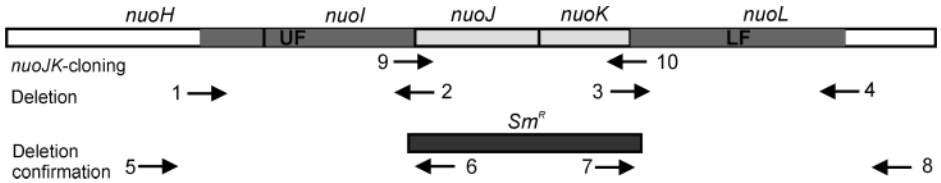

FIGURE 2: Schematic representation of the strategy of *nuoJ* and *nuoK* cloning, deletion from the *E. coli* genome, and verification of their absence from GVnuoJK. The oligonucleotides used for each step and their respective positions within the *nuo* operon are shown. The DNA sequences of the primers are given in Table 2, and technical details are in the Experimental Procedures.

from the assayed membrane sample. Ubiquinone-2 (Q_2) reductase activity was measured in the presence of 20 mM KCN, 100 μM Q_2, and 40 mM MES, pH 6.5. Membranes (30−130 μg of protein) were added to the cuvette containing the reaction mixture described above, and after 30 s of incubation in the presence of the electron acceptor and KCN at 30 °C, the reaction was started by the addition of deamino-NADH to a final concentration of 50 μM. The latter was followed after 2−3 min by the addition of the inhibitor annonin to a final concentration of 10 μg/mL. The inhibitor-sensitive rate of deamino-NADH oxidation was taken to represent the NDH-1 activity. Decylubiquinone (DB) reductase assays were conducted similarly, except that Q_2 was replaced with 100 μM DB, and the incubation period before deamino-NADH addition was 3 min. In addition, 400 μM inhibitor VNA was added instead of annonin after recording the initial activity. The ubiquinone reductase activity of the different mutants was not significantly affected by the structure of the hydrophobic side chain of the acceptor, and consequently, the DB reductase rates are not shown.

RESULTS

Deletion of nuoJ and nuoK. The aerobic respiratory chain of *E. coli* is relatively short and well-understood. Several strains that lack individual functional components of this respiratory chain have previously been prepared, and for the current study, we selected GV102 because it lacks the proton-translocating *bo*-type terminal oxidase (Table 1) and carries only the nonproton-translocating terminal oxidase, cytochrome *bd* (*41*). GV102 has an intact *ndh* gene, encoding NDH-2, the smaller and simpler NADH:ubiquinone reductase of *E. coli* (*36*), and this was expected to be essential for aerobic growth of the planned *nuoJ* + *nuoK* deletion mutant on minimal media. NDH-2 is incapable of using deamino-NADH as an electron donor, while NDH-1 can utilize both NADH and deamino-NADH—a useful feature for distinguishing between the two different NADH oxidation activities in the bacterial membranes (*42*).

The *nuoK* gene in the genome of *E. coli* is preceded by *nuoJ*, which encodes the bacterial homologue of the ND6 subunit of complex I. Both genes are rather short, and there is an overlap between the stop codon of *nuoJ* (TGA) and the first ATG of *nuoK*. For this reason, we included *nuoJ* in the *nuoK* deletion construct and removed both genes by homologous recombination. The deleted genes were replaced by a streptomycin-resistance gene, and the resulting *nuoJ* + *nuoK* deletion mutant was named GVnuoJK. The genetic manipulations were performed using rich media, and under these conditions, the deletion mutant grew at almost normal rates. When it was grown in the malate-YE medium previously used to culture *P. denitrificans* (*31*), however, its growth was severely hampered. GVnuoJK reached a final A_{600} of less than 0.2, while the parent strain, GV102, grew to an A_{600} value above 1.0 under such conditions (Figure 3A).

The malate-YE medium contained 1 mg/mL yeast extract, and it is thus possible that the limited growth of the deletion mutant in this medium was not related to its ability to oxidize malate. This possibility was tested by using growth media in which either the malate or the yeast extract concentration was reduced. The results indicated that lowering the amount of yeast extract reduced the final optical density of the culture significantly, while lowering malate concentration had no such effect (not shown). Furthermore, substitution of malate for succinate did not significantly increase the growth of the GVnuoJK mutant (Figure 3B). On the other hand, the deletion mutant grew to high densities when either pyruvate or glycerol was used as the main carbon source in the growth medium (Figure 3C,D). To understand these observations better, we generated the same *nuoJ* + *nuoK* deletion in another strain, GO103 (Table 1). An important difference (although not the only one) between GO103 and GV102 is the type of terminal oxidase in the respiratory chain. In GO103, it is the proton-translocating enzyme cytochrome *bo*, while in GV102, it is the non proton-translocating enzyme cytochrome *bd* (*41*). It was thus interesting to find out that although the growth pattern of the GOnuoJK strain appeared to be somewhat different from that of its parent strain GO103, it did grow to high densities on the malate-containing medium (Figure 4).

NADH and deamino-NADH oxidation rates in membranes isolated from some of the strains and mutants are listed in Table 3. Interestingly, the NADH oxidation rates in the complemented strain GVcJK (see below) and in the GOnuoJK deletion strain were much lower than those in GVnuoJK (Table 3), yet the two former strains grew to high densities in the malate-containing medium, and GVnuoJK did not (Figures 3 and 4).

To further confirm that the inability of GVnuoJK to grow in the malate-YE medium was not due to inadequate NADH oxidation capacity, GVnuoJK was transformed with pHN3, an expression plasmid for NDH-2 (*36*). Upon induction of NDH-2 expression from pHN3 by the addition of IPTG, the specific NADH:Q_2 oxidoreduction rate in the membranes increased about 6-fold to 1170 ± 110 nmol min^{-1} mg^{-1} (mean ± SE, $n = 4$) versus 200 nmol min^{-1} mg^{-1}. The expression of NDH-2 in the cytoplasmic membrane was also confirmed by Western blotting with anti-His-tag antibodies (results not shown). Nevertheless, the GVnuoJK + NDH2 cells did not grow in the malate-YE medium any better than untransformed GVnuoJK, regardless of the presence of IPTG (Figure 3A). It may be added here that the effect of the *nuoJ* + *nuoK* deletion on the growth of GV102 derivatives in the malate-YE medium came as a surprise to us, and it

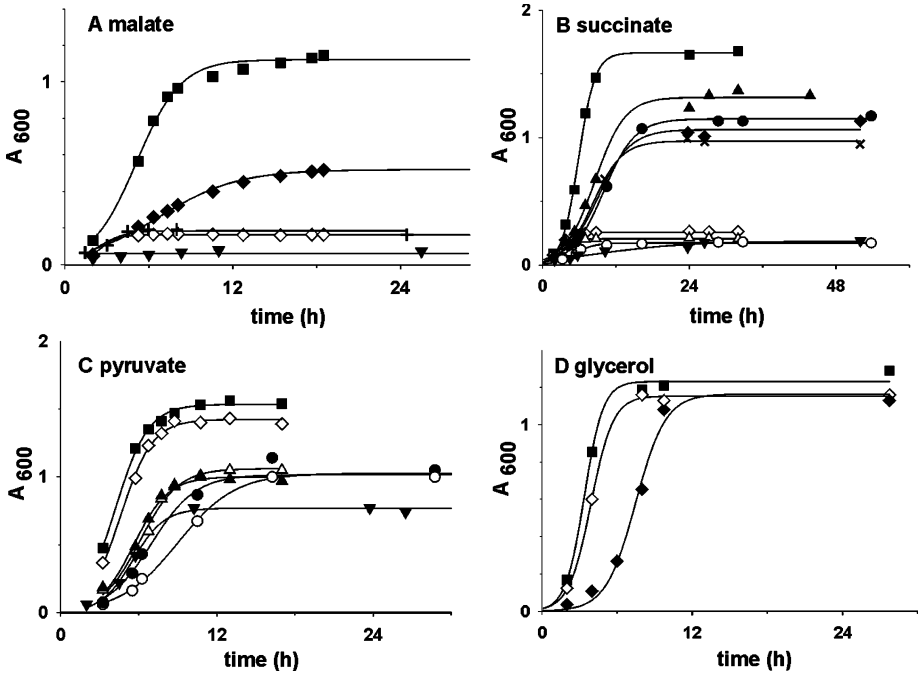

FIGURE 3: Bacterial growth in different media. The strains were grown overnight in LB in the presence of antibiotics and subsequently diluted 1:100 in fresh minimal medium supplemented with 0.1% (w/v) yeast extract (and ampicillin in the presence of complementation plasmids) with the following additions: panel A, 90 mM DL-malate; panel B, 45 mM succinate; panel C, 45 mM pyruvate; and panel D, 15 mM glycerol. Symbols: (■) GV102, (◇) GVnuoJK, (+) GVnuoJK-NDH2 upon IPTG induction, (×) GVcJKwt, (◆) GVcJK, (▲) GVcJK(E36D), (△) GVcJK(E36Q), (●) GVcJK(E72D), (○) GVcJK(E72Q), and (▼) GVcJK(QDDQ).

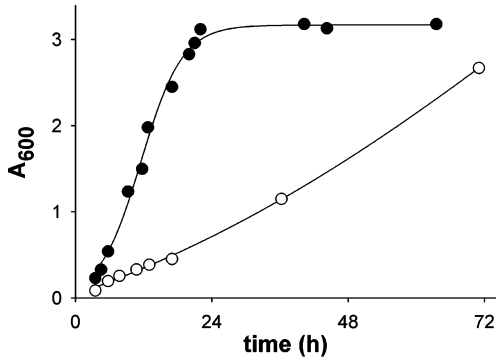

FIGURE 4: Growth of GO103 and GOnuoJK in the malate-YE medium. Experimental conditions were as in Figure 3. (●) GO103 and (○) GOnuoJK.

subsequently turned out to be a useful and simple way of screening the new NDH-1 mutants.

NuoJ + nuoK Complementation. Complementation of the *nuoJ + nuoK* gene deletion was performed in trans by transforming competent GVnuoJK or GOnuoJK cells with pETBlue-2 expression plasmid derivatives containing both genes. To enable easy immuno-detection of NuoK and provide a potentially useful means of purifying NDH-1 by affinity chromatography, we used a *nuoK* gene with a 3′-end extension encoding a 26 amino acid C-terminal tail composed of the Myc epitope followed by six His residues (His-tag, see Experimental Procedures for details). It may be noted here that no mutations were introduced into the *nuoJ* gene in this study and that wild type *nuoJ* was present whenever a mutant form of *nuoK* was expressed. The first complementation was performed using plasmid pJK in which the *nuoK* gene product carried the C-terminal extension described previously. This control complementation of GVnuoJK (yielding GVcJK) restored good growth in either malate-YE or equivalent succinate-containing medium (Figure 3A,B) and increased the inhibitor-sensitive deamino-NADH oxidation activity in the membranes (Table 3). The possible effect of the C-terminal tail on enzymatic activities was tested by complementing the deletion strain with a construct (GVcJKwt) containing the *nuoK* gene without the 3′ extension. The growth (see Figure 3B) and activity values in this case (47±2 nmol min^{-1} mg^{-1} (mean ± SE) for Q_2 reductase activity and 798±37 nmol min^{-1} mg^{-1} for HAR reductase activity) were almost identical to those obtained with the longer subunit (compare with GVcJK in Tables 4 and 5). In light of these results, all the following complementations were performed using the His-tagged NuoK.

Site-Directed Mutations. In the first round of mutagenesis, the two highly conserved acidic residues in the middle of the putative trans-membrane helices 2 and 3 of the NuoK subunit of *E. coli* NDH-1 (Figure 5) were replaced by either Gln or Asp. The effects of these mutations in the GVnuoJK background on bacterial growth and enzymatic activities are presented in Figure 3 and Table 4. It may be noted here that all of the positive growth mutant strains grew well above an A_{600} of 0.3, so that it was easy to discriminate between positive and negative growth phenotypes for all the mutants described in this study. As in the malate-containing medium, GVcJK(E36Q) and GVcJK(E72Q) were unable to grow to higher densities (A_{600}) than 0.3 with succinate, while GVcJK-(E36D) and GVcJK(E72D) grew very well (Figure 3B). Nevertheless, the growth of all these four mutants on pyruvate was good and practically identical (Figure 3C).

The second round of mutagenesis was aimed at examining the importance of the location of the acidic residues along the putative trans-membrane helices 2 and 3 of NuoK. The expectation from the homology between NuoK and HyfE

Table 3: Respiratory Chain Activities in Membranes from Strains and Mutants Grown in a Malate-YE Medium[a]

strain	NADH oxidation (nmol min^{-1} mg^{-1})	d-NADH oxidation		d-NADH:Q_2[b] (nmol min^{-1} mg^{-1})	growth[d]
		nmol min^{-1} mg^{-1}	% inhibition[c]		
GV102	609 ± 60	517 ± 32	99	571 ± 57	+
GVnuoJK	200 ± 25	3 ± 2	nd[e]	0.4 ± 0.3	−
GVnuoJK-NDH2	325 ± 16	nd	nd	nd	−
GVcJK	93 ± 10	54 ± 6	92	74 ± 5	+
GO103	279 ± 48	81 ± 1	100	nd	+
GOnuoJK	40 ± 2	6 ± 2	nd	nd	+
GOcJK	95 ± 6	30 ± 2	nd	nd	+

[a] Values are means ± SE of three to four independent measurements except for the d-NADH oxidation rates in GV102 and GO103, where mean ± range from two measurements is shown. [b] Annonin-sensitive activity. [c] Inhibition by annonin at 10 μg/mL. [d] Negative growth is defined here as an optical density of the culture (A_{600}) below 0.2 after 1 day. [e] nd, not determined.

Table 4: NDH-1 Activities of Cytoplasmic Membranes from GV102 and Its Derivatives Grown on LB Medium

Strain / mutant	Acidic residues[a]	NDH-1 activity[b] nmol·min^{-1}·mg^{-1}	Inhibitor sensitivity (%)[c]	Malate growth[d]	Strain / mutant	Acidic residues[a]	NDH-1 activity[b] nmol·min^{-1}·mg^{-1}	Inhibitor sensitivity (%)[c]	Malate growth[d]
GV102	36E E72	102±2	84	+	A69D	36E E72 D69	51±9	83	+
GVnuoJK		3.1±0.9	10	-	E36Q/E72Q	36Q Q72	2.0±0.5	37	-
GVcJK[e]	36E E72	43±2	80	+	E36Q/I39D	36Q 39D E72	9±2	61	-
E36Q	36Q E72	3.4±0.9	37	-	E36Q/A69D	36Q E72 D69	39±1	87	+
E36D	36D E72	52±3	78	+	E72Q/I39D	36E 39D Q72	74±8	85	+
E72Q	36E Q72	33±2	82	-	E72Q/A69D	36E Q72 D69	33±1	87	-
E72D	36E D72	43±9	78	+	E72Q/G34D	D34 36E Q72	33±2	79	-
I39D	36E 39D E72	60±2	85	+	QDDQ[f]	36Q 39D Q72 D69	88±2	85	-

[a] The positions of the acidic residues and the point mutations along helices 2 and 3 of NuoK are shown schematically. [b] Annonin-sensitive d-NADH:Q_2 activity presented as means ± SE of at least three independent measurements. [c] Percentage inhibition by 10 μg/mL of annonin. [d] Minus sign means A_{600} < 0.2 after 1 day. [e] GVcJK refers to the GVnuoJK deletion strain complemented with the pJK plasmid. This is the control strain for the NuoK mutants. [f] QDDQ refers to the NuoK quadruple mutant E36Q/I39D/A69D/E72Q.

was that simultaneous shifting of both acidic residues, not just one of them at a time, toward the periplasmic side of the helix by approximately one turn (according to the membrane folding reported by Kao et al. (*33*)) would rescue the phenotype of poor growth on malate. To this end, Asp residues were inserted into NuoK that already carried either the E36Q or the E72Q mutation. Furthermore, we also used the mutants to test the effect of placing two acidic residues on the same helix rather than on adjacent ones. The results, presented in Table 4, included some unexpected findings. Insertion of an acidic residue three places downstream of the E36Q mutation did not restore growth on malate when the second acidic residue was the original E72, that is, the mutant was GVcJK(E36Q/I39D), and the same also held good for the mirror image on helix 3, that is, mutant GVcJK-(E72Q/A69D) (Table 4). On the other hand, and in contrast to the original expectations, when both acidic residues were placed on the same helix, either helix 2 or 3, that is, mutants GVcJK(E36Q/A69D) (so that the acidic residues were D69 and E72) and GVcJK(E72Q/I39D) (so that the acidic residues were E36 and D39, Figure 5), the growth on malate was good and similar to that of GVcJK (Table 4). Replacement

Table 5: Deamino-NADH-hexammineruthenium (HAR) Reductase Activity in Membranes from GV102 and Different Mutants Grown on LB Medium

strain/mutant	HAR reduction[a] (nmol min^{-1} mg^{-1})	strain/mutant	HAR reduction[a] (nmol min^{-1} mg^{-1})
GV102	593 ± 50	A69D	440 ± 24
GVnuoJK	163 ± 11	E36Q/E72Q	461 ± 9
GVcJK[b]	724 ± 15	E36Q/I39D	549 ± 65
E36Q	689 ± 23	E36Q/A69D	374 ± 25
E36D	852 ± 46	E72Q/I39D	393 ± 37
E72Q	364 ± 12	E72Q/A69D	666 ± 44
E72D	547 ± 18	E72Q/G34D	435 ± 23
I39D	610 ± 38	QDDQ[c]	855 ± 53

[a] The values are means ± SE of at least three measurements. [b] GVcJK refers to the GVnuoJK deletion strain complemented with plasmid pJK. [c] QDDQ is the quadruple mutant E36Q/I39D/A69D/E72Q.

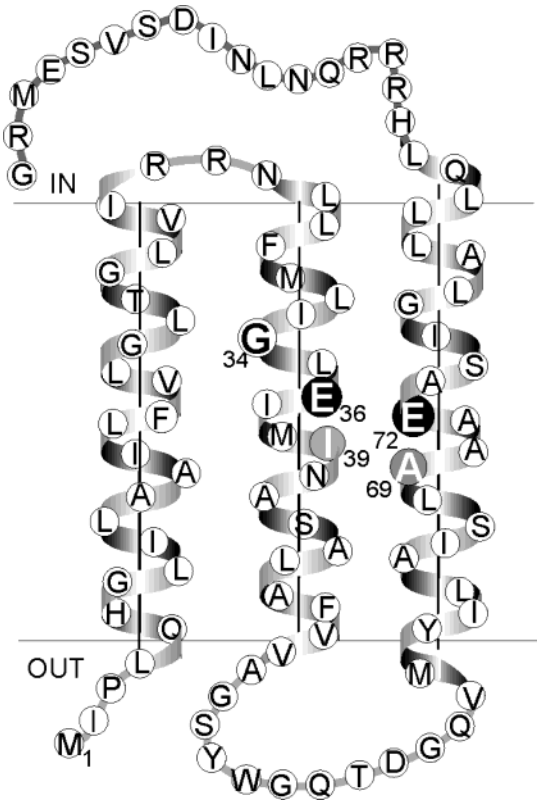

FIGURE 5: Predicted folding of the trans-membrane helices of NuoK in the phospholipid bilayer. The residues subjected to mutation in this work are highlighted, enlarged, and provided with residue numbers.

of Asp with Glu in the latter mutant, that is, GVcJK(E72Q/I39E), resulted in a similar growth phenotype and enzyme activity (not shown).

In the process of sequencing to verify the correctness of the designed mutations, we detected one mutation, G34D/E72Q, that probably occurred during PCR amplification. This appeared to be an interesting test case since its acidic residue, D34, is likely to be oriented in the opposite direction from the original E36 with respect to the normal of the membrane (Figure 5). The plasmid carrying this mutation was thus used to complement the deletion strain, and the resulting mutant, GVcJK(E72Q/G34D), was analyzed. It exhibited a negative growth phenotype in the malate-YE medium, and its NDH-1 activity was low (Table 4).

In addition to single and double mutants, we also prepared a quadruple mutant in which the two acidic residues were

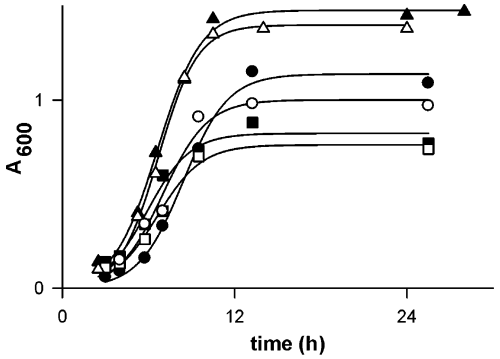

FIGURE 6: Effect of selected complementation plasmids on the growth of the parent strain GV102. The GV102 strain was transfected with plasmids pETBlue-2 (empty plasmid), pJK, or pQDDQ, and growth of the resulting strains was measured in both malate-YE and succinate-YE media. The growth conditions were as in Figure 3. Symbols: (▲) GV102pETBlue-2 in succinate-YE, (●) GV102pJK in succinate-YE, (■) GV102pQDDQ in succinate-YE, (△) GV102pETBlue-2 in malate-YE, (○) GV102pJK in malate-YE, and (□) GV102pQDDQ in malate-YE.

shifted to the positions where HyfE has acidic residues (Figure 1). In the framework of NuoK, this mutant can be written as E36Q/I39D/A69D/E72Q, and it is referred to hereafter as QDDQ. At the outset of this work, such a mutant was expected to restore the enzymatic activity that may be lost by separately shifting the acidic residue in either helix 2 or helix 3 toward the periplasmic side of the membrane by about one turn of the helix. Nevertheless, mutant GVcJK-(QDDQ) did not grow in the malate-YE medium, and it was consequently assumed that the ubiquinone reductase activity of QDDQ is at best similar to that of GVcJK(E72Q), the mutant that exhibited the highest rate of deamino-NADH:ubiquinone reductase activity among the strains that failed to grow on malate (Table 4). It was thus surprising to discover that GVcJK(QDDQ) exhibited a high rate of inhibitor-sensitive deamino-NADH:Q_2 reductase activity, the highest measured for any of the mutants prepared in this study (Table 4). These results prompted us to verify that the poor growth of this mutant in malate-YE medium is not the result of an adverse effect of the mutation other than a low turnover rate of NDH-1. To test this, the parent strain, GV102, was transformed with the QDDQ complementation plasmid, and its growth was examined. These cells grew well in both the malate-YE and the succinate-YE media (Figure 6), almost at same rate as GV102 that was transformed with the wild-type (pJK) plasmid, indicating that the expressed QDDQ mutant protein is not poisonous to the cells. The small difference between growth of GV102 cells that were transformed with pQDDQ or pJK may be explained by the incorporation of some of the mutant subunits into the NDH-1 in GV102pQDDQ cells, thus reducing their energy transduction efficiency (see below). It may also be noted that the GVcJK(QDDQ) mutant grew well on pyruvate (Figure 3C), further supporting the notion that the QDDQ mutant subunit itself does not exert a toxic effect. Hence, the unique combination of poor growth and high activity in the case of GVcJK(QDDQ) may indicate that this mutation lowered the energy conservation efficiency of the enzyme. The implications of these results are discussed below.

It might be argued that the main reason for the differences in growth phenotypes and deamino-NADH oxidation rates among the mutants is the NDH-1 expression level rather than

the catalytic activity of a unit of the mutant enzyme. To examine this possibility, we tested the deamino-NADH:HAR reductase activity in the membranes since this short-cut activity may give an indication of the NDH-1expression level (*43*). The deletion strain, GVnuoJK, exhibited considerable deamino-NADH:HAR reductase activity but significantly less than in the parent strain GV102 (Table 5). Further studies may be needed to clarify whether the HAR reductase activity of GVnuoJK is catalyzed by a membrane-bound subcomplex of *E. coli* NDH-1. In any case, all the complemented strains, including those that did not grow on malate or succinate, exhibited at least twice the rate of HAR reduction that was found in the deletion strain GVnuoJK (Table 5). Furthermore, some mutants that failed to grow to high densities on malate (e.g. GVcJK(E36Q) and GVcJK(QDDQ) (Table 4)) exhibited higher specific HAR reductase activity than GV102 or the mutants GVcJK(E72Q/I39D) and GVcJK(E36Q/A69D), which did grow in the malate-YE medium (Table 5). Hence, a low expression level can be ruled out as the major reason for the growth and activity results obtained here.

DISCUSSION

The folding prediction of the NuoK subunit of NDH-1 of *E. coli*, a homologue of ND4L, a mitochondrially encoded subunit of complex I, indicated the possible location of two Glu residues in the middle of the trans-membrane α-helices (Figure 1). This uncommon placement of acidic residues and their predicted presence in close proximity to each other (Figure 5) may suggest that these glutamates play an important role in the function and/or structure of the enzyme. The present results demonstrate the requirement for two acidic residues in this region of complex I and reveal both limitations and degrees of freedom regarding the exact location of such residues within the membrane-embedded domain of the enzyme.

Growth yields of bacteria in the presence of succinate as the main carbon and energy source have been used previously to determine the proton translocation efficiency of *E. coli* F_1F_o-ATPase (e.g., see ref *44*). The link between proton translocation and growth under these conditions was the depression of dicarboxylate transporter (DctA) transcription due to the low level of cellular ATP (*45*). We report here that a NuoJ + NuoK deletion strain, which also lacks active cytochrome *bo*, was unable to grow on malate or succinate, while growth on a rich medium, or on pyruvate or glycerol as the major carbon source, was practically normal (Figure 3). In line with previous findings (*45*), it is assumed that the poor growth of the new NDH-1 mutants on either malate or succinate media reflects a low level of ATP inside the cells and hence low energy conservation efficiency for the mutant in question. Strong support for this assumption is provided by the growth results obtained with the second nuoJK deletion strain that we prepared (i.e., GOnuoJK). The parent strain for the latter deletion, GO103, differs from GV102, the parent strain for GVnuoJK, in the type of active terminal quinol oxidase in the respiratory chain. In GO103, this oxidase is cytochrome *bo*, the energy conservation efficiency of which is twice as large as that of cytochrome *bd*, the terminal oxidase in GV102 and its derivatives (*41*). It is thus suggested that all the NDH-1 mutants that failed to grow to an optical density higher than 0.2 at 600 nm in the malate-YE medium suffered from insufficient energy transduction along the span from NADH to molecular oxygen.

One possible reason for the low energy yield of the respiratory chain of the NDH-1 mutants could be a poor enzyme turnover rate; thus, even if the proton-translocation stoichiometry of the enzyme was unaffected, the proton pumping rate would be too slow to maintain the electrochemical gradient across the membranes that is needed for ATP synthesis (kinetic effect). Another possible reason is uncoupling or decoupling of the ubiquinone reductase activity of the enzyme from proton translocation, or low H^+/e^- stoichiometry. The kinetic effect may explain the low ATP production in the mutants that exhibit low rates of ubiquinone reduction by NDH-1 specific substrates such as deamino-NADH (Table 4), or at least such an explanation cannot be ruled out. However, in the case of GVcJK(QDDQ), which did not grow in the malate-YE medium but exhibited high rates of ubiquinone reductase activity (Table 4), there seems to be a direct effect on the energy conservation efficiency of the enzyme rather than on its turnover rate.

Replacing either of the conserved Glu residues by Gln (i.e., generating mutants GVcJK(E36Q) and GVcJK(E72Q)) abolished growth on malate or succinate (Table 4). On the other hand, mutants GVcJK(E36D) and GVcJK(E72D) grew well on malate and exhibited similar, or even higher, rates of ubiquinone reductase activity than the control mutant, GVcJK (Table 4). These results indicate that the acidic functions at these particular sites of NDH-1 are important but that the exact length of the amino acid side chain is not.

We tried to rescue the Gln mutant at either the 36 or the 72 positions by inserting an Asp residue three positions upstream or downstream of the original locations of the conserved Glu residues. However, the addition of the second acidic residue at such locations (i.e., generating mutants GVcJK(E36Q/I39D) and GVcJK(E72Q/A69D)) neither restored growth on malate nor significantly improved the ubiquinone reductase activity of the respective single E to Q mutation (Table 4). These double mutants were prepared in two rounds, and we also examined the growth and activity of the intermediate mutants that carried the original two Glu residues at positions 36 and 72 together with an additional Asp at either position 39 (mutant I39D) or 69 (A69D). Both these triple-acidic residue mutants grew on malate [final A_{600} of 0.4 for GVcJK(I39D) and 0.35 for GVcJK(A69D)] and exhibited high rates of Q_2 reductase activity (Table 4). It thus appears that this membrane-embedded domain of NDH-1 can accommodate three as well as two acidic residues.

At the outset of this work, it was considered that the two conserved Glu residues might have a structural role, for example, in keeping the two helices at a given distance and orientation with respect to each other. This idea was examined by constructing two double mutants, E36Q/A69D and E72Q/I39D, in which the two acidic residues were situated on the same helix rather than on opposite ones (Figures 1 and 5). In light of the negative growth phenotype observed for GVcJK(E36Q/I39D) and GVcJK(E72Q/A69D), the positive growth on malate and the relatively high ubiquinone reductase activity of mutants GVcJK(E36Q/A69D) and GVcJK(E72Q/I39D) were unexpected. These results emphasize the need for two acidic residues within this domain and at the same time demonstrate that the two

acidic residues could be located on the same helix and thus probably do not have the structural role suggested above. This does not entirely exclude a structural role other than the one outlined above, but the results are more in accord with the idea that the conserved acidic residues in this domain play an important role in the function of the enzyme.

Little is currently known about the exact role of hydrogenase 4 of *E. coli*, the enzyme that is encoded by the Hyf operon (*34*). A recent report has suggested that it may be involved in ion transport, an interesting possibility with respect to the homology to NDH-1 (*46*). However, the functional relevance of the similarity and difference between the membrane regions of NDH-1 and hydrogenase 4 must await further experimental results. By constructing the quadruple mutant, GVcJK(QDDQ), we planned to generate a HyfE-like situation within NuoK of *E. coli* NDH-1 (Figure 1A) and hoped to reverse the poor growth on malate of mutants GVcJK(E36Q/I39D) and GVcJK(E72Q/A69D). The latter was not achieved since GVcJK(QDDQ) did not grow on the malate-YE medium (Figure 3), but its inhibitor-sensitive deamino-NADH:Q_2 reductase activity was very high (Table 4). Taking these results into account, it is reasonable to suggest that GVcJK(QDDQ) has a significantly lower H^+/e^- stoichiometry than native NDH-1.

One possible reason for the proposed low energy conservation efficiency might be a change in the distance between the pair of acidic residues and another, as yet unknown, important group on the path of the translocated protons through the enzyme. It is premature to speculate on the exact details of this suggestion in the absence of additional structural information, but it may be noted that if the electron transfer in this mutant is fully or partially decoupled from proton pumping, then the results support the suggestions (*6*, *8*) of a conformational change or a similar indirect coupling mechanism between ubiquinone reduction and proton translocation. The alternative mechanism, direct involvement of the ubiquinone reduction chemistry in proton translocation in a way that resembles the Q-cycle in reverse (*47*, *48*), is not supported by the results obtained from the GVcJK-(QDDQ) analyses.

ACKNOWLEDGMENT

We are indebted to Mrs. Maija-Leena Lehtonen for her skilful technical assistance.

REFERENCES

1. Walker, J. E. (1992) *Q. Rev. Biophys. 25*, 253−324.
2. Finel, M. (1998) *Biochim. Biophys. Acta 1364*, 112−121.
3. Dupuis, A., Chevallet, M., Darrouzet, E., Duborjal, H., Lunardi, J., and Issartel, J. P. (1998) *Biochim. Biophys. Acta 1364*, 147−165.
4. Friedrich, T. (1998) *Biochim. Biophys. Acta 1364*, 134−146.
5. Yagi, T., Yano, T., Di Bernardo, S., and Matsuno-Yagi, A. (1998) *Biochim. Biophys. Acta 1364*, 125−133.
6. Brandt, U., Kerscher, S., Drose, S., Zwicker, K., and Zickermann, V. (2003) *FEBS Lett. 545*, 9−17.
7. Dupuis, A., Prieur, I., and Lunardi, J. (2001) *J. Bioenerg. Biomembr. 33*, 159−168.
8. Friedrich, T. (2001) *J. Bioenerg. Biomembr. 33*, 169−177.
9. Vinogradov, A. D. (2001) *Biochemistry (Moscow) 66*, 1086−1097.
10. Yagi, T., Seo, B. B., Di Bernardo, S., Nakamaru-Ogiso, E., Kao, M. C., and Matsuno-Yagi, A. (2001) *J. Bioenerg. Biomembr. 33*, 233−242.
11. Yano, T. (2002) *Mol. Aspects Med. 23*, 345−368.
12. Carroll, J., Shannon, R. J., Fearnley, I. M., Walker, J. E., and Hirst, J. (2002) *J. Biol. Chem. 277*, 50311−50317.
13. Chomyn, A., Cleeter, M. W., Ragan, C. I., Riley, M., Doolittle, R. F., and Attardi, G. (1986) *Science 234*, 614−618.
14. Fearnley, I. M., Carroll, J., Shannon, R. J., Runswick, M. J., Walker, J. E., and Hirst, J. (2001) *J. Biol. Chem. 276*, 38345−38348.
15. Finel, M. (1993) *J. Bioenerg. Biomembr. 25*, 357−366.
16. Man, P. Y., Turnbull, D. M., and Chinnery, P. F. (2002) *J. Med. Genet. 39*, 162−169.
17. Guenebaut, V., Schlitt, A., Weiss, H., Leonard, K., and Friedrich, T. (1998) *J. Mol. Biol. 276*, 105−112.
18. Sled, V. D., Friedrich, T., Leif, H., Weiss, H., Meinhardt, S. W., Fukumori, Y., Calhoun, M. W., Gennis, R. B., and Ohnishi, T. (1993) *J. Bioenerg. Biomembr. 25*, 347−356.
19. Yagi, T., Yano, T., and Matsuno-Yagi, A. (1993) *J. Bioenerg. Biomembr. 25*, 339−345.
20. Dupuis, A., Peinnequin, A., Darrouzet, E., and Lunardi, J. (1997) *FEMS Microbiology Lett. 148*, 107−114.
21. Arkin, I. T., and Brunger, A. T. (1998) *Biochim. Biophys. Acta 1429*, 113−128.
22. Jones, D. T., Taylor, W. R., and Thornton, J. M. (1994) *FEBS Lett. 339*, 269−275.
23. Adelroth, P., Ek, M. S., Mitchell, D. M., Gennis, R. B., and Brzezinski, P. (1997) *Biochemistry 36*, 13824−13829.
24. Fetter, J. R., Qian, J., Shapleigh, J., Thomas, J. W., Garcia-Horsman, A., Schmidt, E., Hosler, J., Babcock, G. T., Gennis, R. B., and Ferguson-Miller, S. (1995) *Proc. Natl. Acad. Sci. U.S.A. 92*, 1604−1608.
25. Hoppe, J., Schairer, H. U., and Sebald, W. (1980) *FEBS Lett. 109*, 107−111.
26. Thomas, J. W., Puustinen, A., Alben, J. O., Gennis, R. B., and Wikström, M. (1993) *Biochemistry 32*, 10923−10928.
27. Verkhovskaya, M. L., Garcia-Horsman, A., Puustinen, A., Rigaud, J. L., Morgan, J. E., Verkhovsky, M. I., and Wikström, M. (1997) *Proc. Natl. Acad. Sci. U.S.A. 94*, 10128−10131.
28. Amarneh, B., and Vik, S. B. (2003) *Biochemistry 42*, 4800−4808.
29. Fisher, N., and Rich, P. R. (2000) *J. Mol. Biol. 296*, 1153−1162.
30. Gong, X., Xie, T., Yu, L., Hesterberg, M., Scheide, D., Friedrich, T., and Yu, C. A. (2003) *J. Biol. Chem. 278*, 25731−25737.
31. Zickermann, V., Barquera, B., Wikström, M., and Finel, M. (1998) *Biochemistry 37*, 11792−11796.
32. Di Bernardo, S., Yano, T., and Yagi, T. (2000) *Biochemistry 39*, 9411−9418.
33. Kao, M. C., Di Bernardo, S., Matsuno-Yagi, A., and Yagi, T. (2002) *Biochemistry 41*, 4377−4384.
34. Andrews, S. C., Berks, B. C., McClay, J., Ambler, A., Quail, M. A., Golby, P., and Guest, J. R. (1997) *Microbiology 143 (Pt 11)*, 3633−3647.
35. Oden, K. L., DeVeaux, L. C., Vibat, C. R., Cronan, J. E., Jr., and Gennis, R. B. (1990) *Gene 96*, 29−36.
36. Björklöf, K., Zickermann, V., and Finel, M. (2000) *FEBS Lett. 467*, 105−110.
37. Link, A. J., Phillips, D., and Church, G. M. (1997) *J. Bacteriol. 179*, 6228−6237.
38. Raito, M., and Wikström, M. (1994) *Biochim. Biophys. Acta 1186*, 100−106.
39. Leif, H., Sled, V. D., Ohnishi, T., Weiss, H., and Friedrich, T. (1995) *Eur. J. Biochem. 230*, 538−548.
40. Lowry, O. H., Rosebrough, N. J., Farr, A. L., and Randall, R. J. (1951) *J. Biol. Chem. 193*, 265−275.
41. Puustinen, A., Finel, M., Haltia, T., Gennis, R. B., and Wikström, M. (1991) *Biochemistry 30*, 3936−3942.
42. Matsushita, K., Ohnishi, T., and Kaback, H. R. (1987) *Biochemistry 26*, 7732−7737.
43. Zickermann, V., Kurki, S., Kervinen, M., Hassinen, I., and Finel, M. (2000) *Biochim. Biophys. Acta 1459*, 61−68.
44. Miller, M. J., Oldenburg, M., and Fillingame, R. H. (1990) *Proc. Natl. Acad. Sci. U.S.A. 87*, 4900−4904.
45. Boogerd, F. C., Boe, L., Michelsen, O., and Jensen, P. R. (1998) *J. Bacteriol. 180*, 5855−5859.
46. Bagramyan, K., Vassilian, A., Mnatsakanyan, N., and Trchounian, A. (2001) *Membr. Cell Biol 14*, 749−763.
47. Brandt, U. (1997) *Biochim. Biophys. Acta 1318*, 79−91.
48. Dutton, P. L., Moser, C. C., Sled, V. D., Daldal, F., and Ohnishi, T. (1998) *Biochim. Biophys. Acta 1364*, 245−257.

BI0355903